Scientific Research Publishing

Circuits and Systems, 2026, 17(5), 83-114
https://www.scirp.org/journal/cs
ISSN Online: 2153-1293
ISSN Print: 2153-1285

Comprehensive Assessment of Large-Scale Photovoltaic Integration in an Isolated Mining Microgrid: Dynamic Stability, Protection Coordination, and Power Quality Analysis

Medhy Kayembe Kazadi*, Narcisse Meni Babakidi*

Department of Electrical Engineering, Institut Supérieur des Techniques Appliquées, Kolwezi, Democratic Republic of the Congo
Email: *kayembemedy@gmail.com, *narcisse.meni@ista.ac.cd

How to cite this paper: Kazadi, M.K. and Babakidi, N.M. (2026) Comprehensive Assessment of Large-Scale Photovoltaic Integration in an Isolated Mining Microgrid: Dynamic Stability, Protection Coordination, and Power Quality Analysis. *Circuits and Systems*, **17**, 83-114.
https://doi.org/10.4236/cs.2026.175005

Received: April 27, 2026
Accepted: May 26, 2026
Published: May 29, 2026

Abstract

The decarbonization of isolated mining operations has accelerated the adoption of large-scale photovoltaic (PV) generation as a sustainable alternative to diesel-based electricity production. However, high PV penetration in isolated microgrids introduces significant technical challenges, including reduced system inertia, voltage and frequency instability, protection coordination, fault-current variation, and power quality degradation. This study presents a comprehensive technical assessment of integrating a 15 MW photovoltaic power plant into the isolated electrical network of the Société Minière de Dinguiraye (SMD) gold mine in Guinea using ETAP Version 22.5. A high-fidelity digital model of the mining power system was developed, incorporating diesel generators, medium-voltage distribution networks, transformers, industrial loads, photovoltaic generation, advanced inverter controls, protection systems, and an optional Battery Energy Storage System (BESS). Five representative operating scenarios were investigated through load-flow, transient stability, short-circuit, protection coordination, harmonic, and renewable intermittency analyses to evaluate the operational performance of the proposed hybrid diesel-PV microgrid. Simulation results demonstrate that the integration of the 15 MW PV plant substantially reduces diesel generation while maintaining acceptable voltage regulation, frequency stability, rotor-angle stability, protection selectivity, and harmonic distortion within the limits specified by IEEE 519. The implementation of advanced inverter control functions and BESS-based fast frequency response further enhances voltage support, improves frequency recovery following disturbances, mitigates renewable intermittency, and increases the overall resilience of the isolated microgrid. The study confirms that large-scale photovoltaic integration can be achieved without compromising system reliability, operational security, or power quality when supported by appropriate control strategies and protection coordination. The proposed ETAP-based assessment framework provides a practical and reproducible engineering methodology for the planning, design, and implementation of renewable-powered isolated mining microgrids, contributing to the decarbonization and sustainable electrification of remote mining operations.

Keywords

Photovoltaic Integration, Isolated Mining Microgrid, ETAP, Dynamic Stability, Protection Coordination, Power Quality, Battery Energy Storage System (BESS), Renewable Energy, Mining Electrification

1. Introduction

The global mining industry is undergoing a profound energy transition driven by the need to reduce greenhouse gas emissions, improve energy security, and achieve long-term operational sustainability. Many remote mining operations continue to rely on isolated diesel-powered microgrids, where fuel transportation, high operating costs, and carbon emissions represent significant economic and environmental challenges. Consequently, the integration of renewable energy technologies, particularly large-scale photovoltaic (PV) systems, has emerged as an attractive solution for reducing diesel dependency while supporting corporate decarbonization strategies and Environmental, Social, and Governance (ESG) objectives [1] [2].

Among the available renewable technologies, utility-scale photovoltaic generation is particularly well suited to mining applications because of its declining installation costs, modular architecture, low maintenance requirements, and high solar resource availability in many mining regions. However, integrating inverter-based PV generation into isolated industrial power systems introduces several technical challenges. Unlike conventional synchronous generators, photovoltaic systems contribute little rotational inertia and provide limited fault current, thereby affecting voltage regulation, frequency stability, transient performance, protection coordination, and power quality. These challenges become increasingly significant in mining microgrids supplying large induction motors, variable-speed drives (VSDs), crushers, pumps, ventilation systems, conveyors, and other highly dynamic industrial loads. Maintaining reliable operation under high renewable penetration therefore requires coordinated control of inverter-based resources, optimized protection schemes, and, where appropriate, Battery Energy Storage Systems [3] [4].

Although renewable energy integration has been extensively investigated over the past decade, most published studies focus on utility distribution networks, generic islanded microgrids, or simplified academic test systems. Existing research frequently examines individual technical aspects such as voltage regulation, frequency stability, economic optimisation, or harmonic mitigation without simultaneously evaluating the complex interactions among power flow, transient stability, protection coordination, short-circuit performance, and power quality in a real industrial mining environment. Furthermore, comprehensive engineering studies involving large-scale photovoltaic integration (15 MW or greater) within isolated African mining microgrids remain scarce, limiting the availability of practical design guidance for mining operators and power system engineers [5] [6].

To address this gap, this paper presents a comprehensive technical assessment of integrating a 15 MW photovoltaic power plant into the isolated electrical network of the Société Minière de Dinguiraye (SMD) gold mine in Guinea. A high-fidelity digital model of the existing diesel-powered microgrid was developed using ETAP Version 22.5 to represent the complete electrical infrastructure, including diesel generators, transformers, medium-voltage distribution networks, industrial loads, protection systems, photovoltaic generation, and an optional Battery Energy Storage System (BESS). Comprehensive simulation studies were subsequently performed to evaluate load-flow performance, transient stability, frequency response, short-circuit behavior, protection coordination, harmonic distortion, and renewable intermittency under representative operating conditions [7] [8].

The principal contribution of this research is the development of an integrated ETAP-based assessment framework for evaluating large-scale renewable energy integration in isolated mining power systems. Unlike previous studies that focus on individual performance criteria, the proposed methodology simultaneously investigates steady-state operation, dynamic behaviour, protection performance, and power quality within a single validated industrial simulation model. The study demonstrates that high photovoltaic penetration can substantially reduce diesel generation while maintaining electrical stability, operational reliability, protection selectivity, and compliance with internationally recognized engineering standards through the application of advanced inverter control strategies and BESS support [9] [10].

The findings provide both scientific and practical contributions by offering a reproducible engineering methodology for the planning, design, optimisation, and implementation of renewable-powered mining microgrids. The proposed framework serves as a valuable reference for mining companies, utilities, consultants, and researchers involved in the electrification and decarbonization of isolated industrial power systems, particularly in Africa and other remote regions pursuing high renewable energy penetration [11] [12].

2. Literature Review

2.1. Renewable Energy Integration in Isolated Mining Microgrids

The mining sector is increasingly adopting renewable energy technologies to reduce diesel dependency, operating costs, greenhouse gas emissions, and improve long-term energy sustainability. Among the available renewable sources, large-scale photovoltaic (PV) systems have emerged as the preferred solution for isolated mining operations because of declining installation costs, high conversion efficiency, low maintenance requirements, and abundant solar resources. Hybrid diesel-PV microgrids have demonstrated significant reductions in fuel consumption while enhancing environmental performance and supporting corporate decarbonization and ESG objectives [13] [14].

Despite these benefits, integrating inverter-based PV generation into isolated mining power systems presents considerable technical challenges. Unlike conventional synchronous generators, photovoltaic systems provide limited rotational inertia and fault current contribution, fundamentally altering power system dynamics. High PV penetration can therefore affect voltage regulation, frequency stability, transient performance, protection coordination, and power quality, particularly in mining networks characterized by large motor loads, variable-speed drives, and rapidly changing industrial demand [14].

Consequently, advanced inverter control strategies, adaptive protection schemes, and Battery Energy Storage Systems (BESS) have become essential for maintaining reliable and secure operation. ETAP has emerged as one of the most widely adopted simulation platforms for evaluating these challenges through integrated load-flow, transient stability, short-circuit, harmonic, and protection coordination analyses [15].

2.2. Research Gap and Contribution

Although substantial research has been conducted on renewable energy integration, most published studies focus on utility distribution systems, generic microgrids, or simplified academic models. Existing investigations typically examine isolated technical aspects such as voltage regulation, frequency stability, economic optimization, or harmonic performance without simultaneously assessing the complex interactions between power flow, dynamic stability, protection coordination, fault performance, and power quality in real industrial environments. Furthermore, comprehensive studies involving large-scale photovoltaic integration (≥15 MW) in isolated African mining microgrids remain scarce [15] [16].

To address these limitations, this research develops a high-fidelity ETAP-based assessment framework for the isolated electrical network of the Société Minière de Dinguiraye (SMD), a gold mine in Guinea. The proposed methodology integrates steady-state load-flow analysis, transient stability, short-circuit studies, frequency response, harmonic analysis, protection coordination, advanced inverter control strategies, and Battery Energy Storage System (BESS) evaluation within a single simulation environment [16].

Unlike previous studies, this work provides a comprehensive engineering assessment based on a real industrial mining power system, offering practical guidance for the planning, design, optimization, and implementation of reliable, safe, and sustainable renewable-powered mining microgrids. The proposed framework contributes both to the academic literature and to industrial practice by providing a reproducible methodology for evaluating large-scale renewable integration in isolated mining power systems [17].

3. Research Methodology

3.1. Research Design

This study employed a quantitative engineering methodology based on computer-aided power system modelling and simulation to evaluate the technical feasibility of integrating a 15 MW photovoltaic (PV) power plant into the isolated electrical network of the Société Minière de Dinguiraye (SMD), Guinea. The analysis was performed using ETAP Version 22.5, enabling comprehensive steady-state and dynamic assessments of the existing diesel-based microgrid under different renewable penetration scenarios.

A simulation-based approach was selected because it provides a safe and reliable environment for investigating system behavior without interrupting mining operations. The study adopted a Before-After assessment framework, whereby the existing diesel power system was first modelled and validated before progressively introducing photovoltaic generation and Battery Energy Storage System (BESS) support. This approach enabled direct comparison of network performance before and after renewable integration [17] [18].

3.2. Research Framework

The research methodology was structured into six sequential phases to ensure a systematic and reproducible assessment of the proposed hybrid diesel-PV microgrid:

1) Data Collection: Relevant electrical and operational data were collected, including single-line diagrams, generator and transformer characteristics, cable parameters, protection settings, load profiles, and photovoltaic plant specifications.

2) ETAP Network Modelling: A detailed digital model of the SMD electrical network was developed in ETAP, incorporating equipment parameters, load allocation, protection devices, and the validated network topology.

3) Base-Case Validation: The diesel-only model was validated using load-flow results, bus voltage profiles, generator and transformer loading, power factor, network losses, and short-circuit levels to confirm consistency with existing operating conditions.

4) Photovoltaic and BESS Integration: A 15 MW grid-following photovoltaic plant was integrated into the model with advanced inverter functions, including Volt/VAR control, frequency support, ramp-rate limitation, fault ride-through capability, and optional Battery Energy Storage System modelling.

5) Simulation Studies: The hybrid system was evaluated through load-flow, transient stability, short-circuit, protection coordination, harmonic, and renewable intermittency analyses under representative operating scenarios.

6) Performance Evaluation: The diesel-only and hybrid diesel-PV configurations were comparatively assessed using technical performance indicators, leading to engineering recommendations for reliable and practical implementation.

This structured framework enables a comprehensive evaluation of steady-state performance, dynamic stability, protection behavior, and power quality within a single validated simulation environment.

3.3. Study Area

The study was conducted on the isolated electrical network of Société Minière de Dinguiraye (SMD), a Nordgold gold mining operation located in Guinea. The electrical configuration of the SMD isolated mining network is shown in Figure 1.

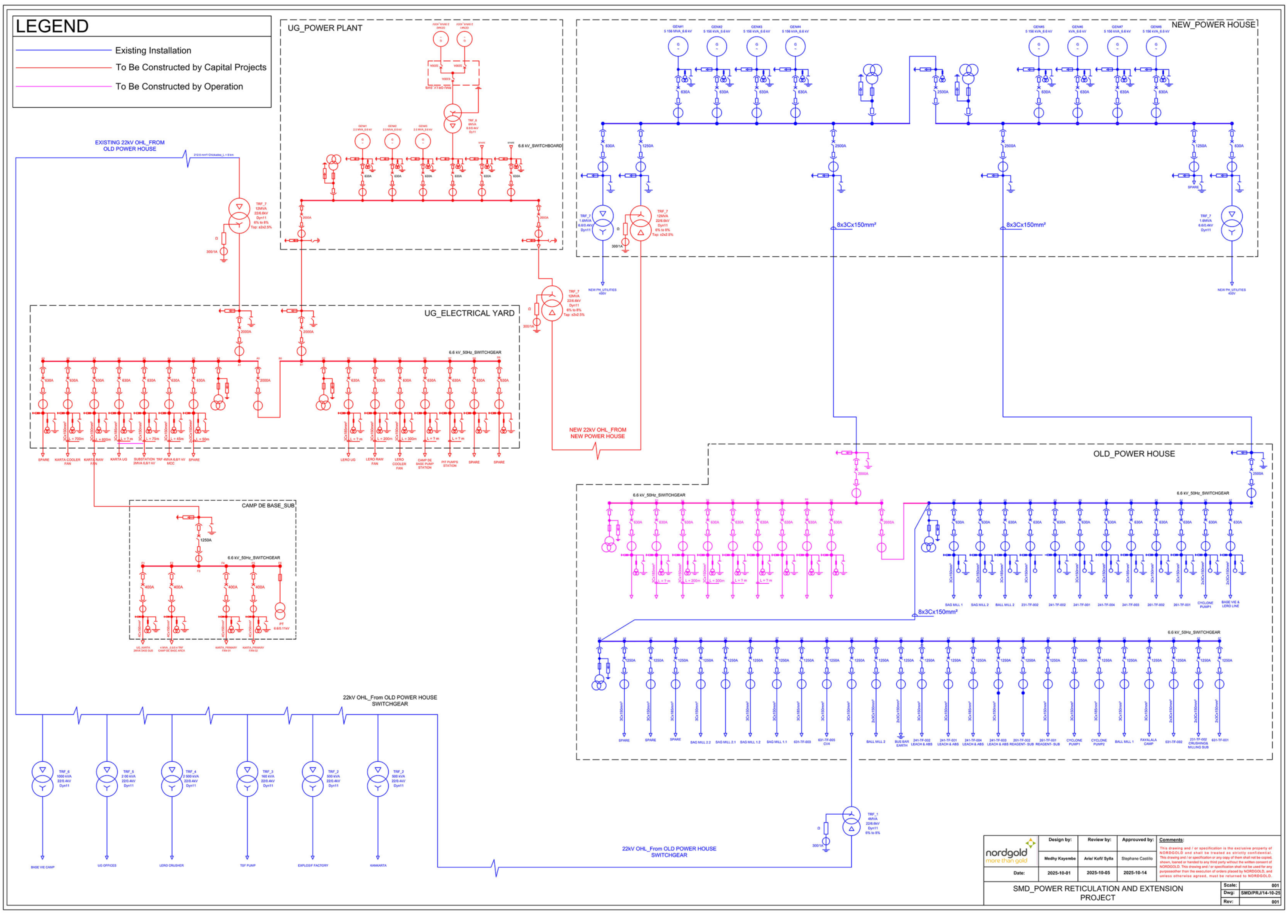

Figure 1. General electrical power distribution network of the SMD mining plant.

The power system operates independently of the national grid and comprises diesel generating units operating at 6.6 kV, a 22 kV distribution network, power transformers, industrial substations, low- and medium-voltage motor control centres (MCCs), underground electrical distribution systems, and critical mining process loads.

As shown in Figure 1, the existing UG power plant comprises five diesel generator sets with a combined installed capacity of 12.5 MVA, configured as follows:

- Three (3) Mitsubishi prime-rated diesel generators, each rated at 2.5 MVA, 6.6 kV, 50 Hz, operating as the primary base-load generation units.
- Two (2) Teksan standby diesel generators, each rated at 2.5 MVA, 400 V, 50 Hz, connected to the 6.6 kV distribution system through dedicated 400 V/6.6kV step-up transformers. These units provide backup generation capacity during maintenance, contingency events, or periods of increased system demand.

The total installed diesel generation capacity is 12.5 MVA, corresponding to approximately 10 MW of active power at a nominal power factor of 0.8. During all ETAP simulations, diesel generator dispatch was constrained within the installed capacity of the online generators. The operating configuration adopted for each simulation case is summarized in Table 1.

The ETAP simulations were performed using four operating configurations. The base case represents the existing diesel-only microgrid, while the remaining cases evaluate the progressive integration of a 15 MW photovoltaic power plant, advanced Volt/VAR control, and Battery Energy Storage System (BESS)-based Fast Frequency Response (FFR). These operating configurations were used consistently across the different load-flow, transient stability, protection coordination, and power quality analyses.

Table 1. Operating configuration used in ETAP simulations.

Simulation case	Online diesel units	Installed genset (MVA)	PV output (MW)	Operating mode	BESS
Case 1 (base case)	3 × Mitsubishi	7.5	0	Diesel-only	No
Case 2	3 × Mitsubishi	7.5	15	Diesel + PV	No
Case 3	3 × Mitsubishi	7.5	15	Diesel + PV with Volt/VAR control	No
Case 4	3 × Mitsubishi	7.5	15	Diesel + PV + Fast frequency response (FFR)	Yes (BESS)

The proposed renewable energy system consists of a 15 MW utility-scale photovoltaic (PV) power plant will be integrated into the existing 6.6 kV underground (UG) power plant distribution network, forming a hybrid diesel-photovoltaic microgrid. The PV plant is connected to the main 6.6 kV busbar through an appropriately rated step-up transformer, allowing seamless integration with the existing power generation infrastructure while ensuring compliance with system voltage and protection requirements.

The operating conditions presented in Table 2 were consistently applied across all simulation scenarios to ensure a fair comparison. The system load was maintained at approximately 8 MW, with three Mitsubishi diesel generators operating online. A minimum diesel loading of 30% and a 15% spinning reserve were maintained to ensure stable islanded operation. For the BESS scenario, a 5 MW/10MWh battery with an initial 60% state of charge (SOC) was modelled to provide Fast Frequency Response (FFR). Steady-state analyses were based on converged load-flow solutions, while transient simulations were performed over a 30-second duration to capture the dynamic response of the hybrid microgrid.

Table 2. Operating conditions used for ETAP simulation scenarios.

Parameter	Case 1 diesel only	Case 2 diesel + PV	Case 3 diesel + PV + Volt/VAR	Case 4 diesel + PV + BESS
Total system load	8.0 MW	8.0 MW	8.0 MW	8.0 MW
Online diesel generators	3 × 2.5 MVA Mitsubishi	3 × 2.5 MVA Mitsubishi	3 × 2.5 MVA Mitsubishi	3 × 2.5 MVA Mitsubishi
Available diesel capacity	7.5 MVA	7.5 MVA	7.5 MVA	7.5 MVA
PV output	0 MW	15 MW	15 MW	15 MW
Minimum diesel loading	30% of rated output per unit	0.3	0.3	0.3
Required spinning reserve	15% of total system load	0.15	0.15	0.15
BESS rated power	—	—	—	5 MW
BESS energy capacity	—	—	—	10 MWh
Initial BESS State of Charge	—	—	—	0.6
Simulation duration (Load Flow)	Steady-state	Steady-state	Steady-state	Steady-state
Simulation duration (Dynamic)	30 s	30 s	30 s	30 s

3.4. ETAP Model Development

A comprehensive digital twin of the mining power system was developed using ETAP Version 22.5. The developed ETAP model of the SMD isolated mining microgrid is illustrated in Figure 3. The model incorporated all major electrical components, including diesel generators, power transformers, medium-voltage switchgear, overhead lines, underground cable networks, induction motors, variable frequency drives (VFDs), photovoltaic generation, Battery Energy Storage Systems (BESS), protection relays, circuit breakers, busbars, and feeders. Equipment parameters were derived from manufacturer technical documentation, engineering design data, and operational records obtained from the mine. Model validation was performed by comparing simulated operating conditions with measured system performance under normal operating conditions, confirming that the digital model accurately represents the actual electrical network prior to photovoltaic integration [18].

As shown in Figure 2, the ETAP model accurately represents the complete electrical topology of the SMD isolated mining power system, including the diesel generating units, medium-voltage distribution network, transformers, industrial loads, photovoltaic generation, Battery Energy Storage System (BESS), and protection devices. This validated digital model served as the basis for all subsequent load-flow, transient stability, short-circuit, protection coordination, and harmonic analyses [18] [19].

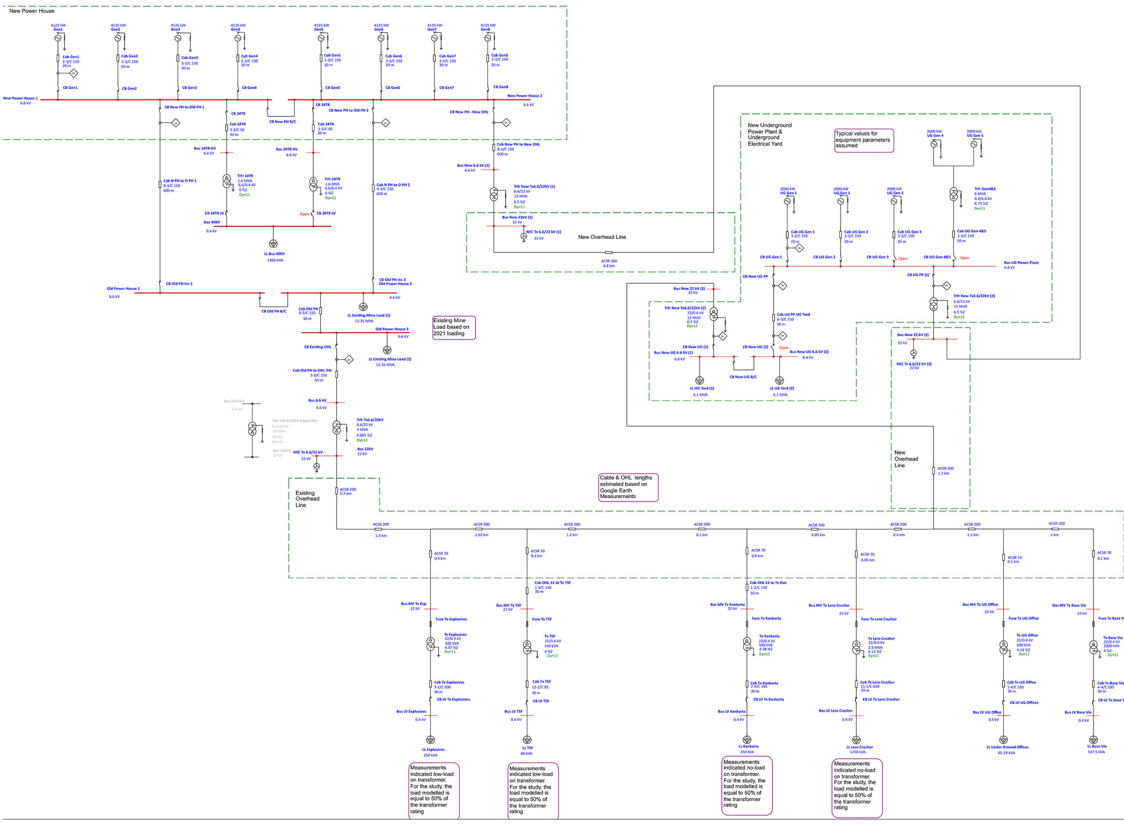

Figure 2. ETAP digital model.

3.5. Photovoltaic and Battery Energy Storage System Modelling

The photovoltaic plant was modelled as a 15 MW grid-following inverter-based generation system connected to the medium-voltage network. The inverter model incorporated active and reactive power control, Volt/VAR regulation, frequency droop characteristics, ramp-rate limitation, low-voltage ride-through (LVRT), high-voltage ride-through (HVRT), and fault-current limitation [19] [20].

As shown in Table 3, the selected modelling parameters were established in accordance with inverter manufacturer recommendations, IEEE 1547, IEC 61727, and ETAP modelling practices to ensure realistic steady-state, transient stability, protection, and power quality simulations. These parameters provide a representative framework for evaluating the dynamic behavior and grid integration performance of the proposed 15 MW photovoltaic power plant within the isolated SMD hybrid diesel-PV microgrid.

To evaluate enhanced operational flexibility, selected simulation scenarios included a Battery Energy Storage System (BESS) providing frequency support, synthetic inertia, active power balancing, renewable intermittency mitigation, voltage support, and ramp-rate control.

Table 3. Reference parameters of the 15 MW photovoltaic power plant (Modeling assumptions).

Parameter	Recommended value	Brief technical comment
Maximum active power	15 MWac	Net power at PCC
Inverter apparent power	≥16.5 MVA	Supports P and Q
Connection voltage	6.6 kV, 50 Hz	Step-up transformer
Inverter type	Grid-following with PLL	Grid synchronized
Nominal power factor	1	Adjustable
Power factor range	0.95 leading to 0.95 lagging	Inverter limited
Reactive power capability	±5 MVAr	Voltage support
Main reactive control	Volt/VAR or PCC voltage control	Voltage regulation
Normal control priority	Active-power priority	Maximizes PV output
Fault control priority	Reactive-current priority	Fault support
Voltage reference	1.00 p.u.	PCC setpoint
Frequency-power droop	0.04	Frequency regulation
Frequency deadband	±0.10 Hz	Avoids unnecessary response
Fault-current limit	1.2 p.u.	Current limited
Voltage-control response time	≤100 ms	Fast response
Frequency-control response time	100 - 200 ms	Dynamic control
Normal ramp-rate limit	10% of rated power/min	Power smoothing
Severe transient ramp scenario	0.5 - 2 MW/s	Disturbance case
Continuous voltage range	0.95 - 1.05 p.u.	Normal operation
Temporary voltage ride-through range	0.85 - 1.10 p.u.	Fault ride-through
Normal frequency range	49 - 51 Hz	Continuous operation
Extreme study range	47.5 - 52 Hz	Protection study
Voltage and frequency ride-through	Defined UVRT/OVRT curves	Grid-code compliant
Harmonic voltage limit at PCC	THDv ≤ 5%	Power quality
Recommended transformer rating	16.5 - 18 MVA	Operating margin
Transformer impedance	6% - 8%	Fault limitation
Grid-forming source	Three Mitsubishi diesel generators	Provides the voltage and frequency reference during islanded operation.

The proposed 15 MW PV plant was modelled as a grid-following inverter synchronized to the diesel-powered microgrid through a Phase-Locked Loop (PLL). The three online Mitsubishi synchronous diesel generators operated in grid-forming mode, establishing the voltage reference through their Automatic Voltage Regulators (AVRs) and regulating system frequency through governor-based droop control. The PV inverter supplied active power and Volt/VAR-based reactive power support while maintaining synchronization with the diesel-generated voltage. In the BESS scenario, the battery provided Fast Frequency Response (FFR) and synthetic inertia through rapid active power injection or absorption in response to frequency deviations and RoCoF. However, the BESS remained coordinated with the diesel generators, which served as the primary grid-forming sources throughout all simulation scenarios, ensuring stable voltage and frequency regulation during both steady-state and transient operation.

3.6. Simulation Study Design and Assessment Scope

Five representative operating scenarios were investigated:

- Load-Flow Analysis: Evaluation of bus voltage profiles, active and reactive power flow, equipment loading, network losses, and power factor.
- Dynamic Stability Analysis: Assessment of frequency response, voltage recovery, rotor angle stability, diesel generator dynamics, and renewable power fluctuations.
- Short-Circuit and Protection Coordination: Analysis of fault currents, relay operating times, breaker coordination, and protection selectivity.
- Harmonic Analysis: Evaluation of voltage and current harmonic distortion, harmonic spectrum, resonance conditions, and filter performance.
- Renewable Intermittency Analysis: Investigation of sudden photovoltaic output reductions, frequency recovery, BESS response, and diesel governor performance under variable solar conditions.

3.7. Technical Performance Indicators and Evaluation Criteria

The technical performance of the hybrid power system was evaluated using internationally recognised electrical performance indicators, including bus voltage magnitude, active and reactive power flow, system frequency, Rate of Change of Frequency (RoCoF), rotor angle stability, short-circuit current, relay operating time, total harmonic distortion (THDv and THDi), power factor, diesel fuel displacement, and renewable penetration level.

Comparative analyses between the reference diesel network and the hybrid diesel-PV system was conducted to quantify the operational benefits and technical impacts of photovoltaic integration [21] [22].

3.8. Standards and Validation

All simulations and engineering assessments were conducted in accordance with internationally recognised standards, including IEC 60909, IEC 61000, IEEE 519, IEEE 1547, IEC 60034, IEC 60255, and IEC 61850. Adherence to these standards ensures methodological consistency, technical reliability, and reproducibility for similar isolated mining microgrids [23].

3.9. Research Workflow

The research followed a systematic workflow comprising data collection, ETAP model development, base-case validation, photovoltaic (PV) and Battery Energy Storage System (BESS) integration, simulation studies, performance evaluation, and the formulation of engineering recommendations.

The ETAP model was first developed and validated using actual operating data before introducing the proposed 15 MW PV power plant and BESS. Comprehensive simulations, including load-flow, transient stability, short-circuit, protection coordination, harmonic, and renewable intermittency analyses, were subsequently performed to assess the technical performance of the hybrid microgrid.

This structured methodology provides a reproducible engineering framework for evaluating renewable energy integration into isolated mining power systems while ensuring electrical stability, operational reliability, protection coordination, power quality, and compliance with international engineering standards [22] [23].

4. ETAP Model and Study System

4.1. Study System Overview

The study was conducted on the isolated electrical network of the Société Minière de Dinguiraye (SMD), a Nordgold mining operation in Guinea. The mine operates as a standalone microgrid powered by diesel generators, supplying industrial loads through 22 kV and 6.6 kV distribution networks. A 15 MW photovoltaic (PV) power plant was proposed for integration into the existing system to reduce diesel fuel consumption while maintaining network reliability.

4.2. Existing Electrical Network

The configuration of the existing SMD electrical network is illustrated in **Figure 1**. The mine operates as an isolated diesel-powered microgrid designed to supply continuous electrical power to critical mining and processing facilities. As shown in **Figure 1**, the network comprises diesel generating units operating at 6.6 kV, interconnected through a 22 kV overhead distribution system, 22/6.6 kV power transformers, medium-voltage switchgear, underground and surface cable networks, industrial substations, and medium- and low-voltage motor control centers (MCCs).

The electrical system supplies a wide range of mining process loads, including SAG mills, crushers, pumps, ventilation fans, conveyors, and auxiliary services, all of which exhibit varying load characteristics and require a high level of operational reliability. The combination of large rotating machines, power electronic drives, and continuously varying industrial loads makes the network representative of a complex isolated mining microgrid and provides an appropriate platform for evaluating the integration of large-scale photovoltaic generation and Battery Energy Storage Systems (BESS) [24] [25].

4.3. ETAP Digital Model

A detailed digital twin of the SMD electrical network was developed using ETAP Version 22.5 to accurately represent the configuration of the isolated mining microgrid shown in **Figure 1**. The corresponding ETAP implementation of the network is presented in **Figure 2**.

The digital model incorporates all major electrical components of the existing power system, including diesel generators, power transformers, 22 kV overhead distribution lines, underground and surface cable networks, medium-voltage switchgear, industrial induction motors, variable frequency drives (VFDs), protection relays, circuit breakers, busbars, feeders, the proposed 15 MW photovoltaic (PV) power plant, and the optional Battery Energy Storage System (BESS). Equipment ratings, electrical characteristics, protection settings, and operational parameters were derived from manufacturer technical documentation, engineering design data, and operational records obtained from the mine to ensure an accurate representation of the actual network [25] [26].

As shown in **Figure 2**, the validated ETAP model served as the foundation for all load-flow, transient stability, short-circuit, protection coordination, and harmonic analyses performed in this study.

4.4. Equipment Modelling

The principal electrical components of the SMD hybrid diesel-PV microgrid were modelled in ETAP using detailed electrical and dynamic parameters to accurately represent their steady-state and transient operating characteristics. Diesel generators were represented by synchronous machine models incorporating governor and Automatic Voltage Regulator (AVR) controls to simulate active power dispatch, frequency regulation, and voltage response under varying operating conditions. Power transformers were modelled using their rated capacity, voltage ratio, vector group, leakage impedance, winding losses, and on-load tap changer settings to ensure accurate voltage transformation and power-flow calculations [27] [28].

Overhead transmission lines and underground cable networks were represented using conductor electrical characteristics, installation configurations, and positive- and zero-sequence impedance parameters to accurately simulate power transfer, voltage drop, fault current levels, and network losses. Industrial loads, including major mining equipment such as SAG mills, crushers, pumps, ventilation fans, and conveyors, were modelled as dynamic induction motor loads to capture their starting characteristics, transient behavior, and reactive power demand. This detailed equipment modelling enabled realistic simulation of both normal operating conditions and network disturbances, thereby providing a reliable basis for load-flow, transient stability, short-circuit, protection coordination, and harmonic analyses [26].

The protection settings presented in **Table 4** were adopted as representative ETAP coordination settings for the 6.6 kV network. Phase and earth-fault protection were implemented using IEC Standard Inverse characteristics in accordance with IEC 60255-151. The settings were selected to maintain adequate sensitivity to feeder faults while preserving discrimination between normal loading, downstream faults, and upstream backup protection. Final field implementation would require verification against the approved SMD protection coordination study, equipment short-circuit withstand ratings, and manufacturer relay setting files.

Table 4. Representative protection settings adopted in the ETAP study.

Parameter	Proposed value
Relay type	CPN500M/CPN500L
Overcurrent characteristic	IEC Standard Inverse
Phase overcurrent pickup, 51P	0.80 A secondary (160 A primary)
Earth-fault pickup, 51N	0.20 A secondary (40 A primary)
Instantaneous phase element, 50P	8.0 A secondary (1600 A primary)
Instantaneous earth-fault element, 50N	2.0 A secondary (400 A primary)
Time Multiplier Setting, 51P	0.1
Time Multiplier Setting, 51N	0.08
Breaker opening time	200 ms
System frequency	50 Hz

4.5. Model Validation

The ETAP digital model was validated against the existing diesel-only operating conditions before introducing the proposed photovoltaic (PV) generation system. Validation was performed by comparing simulated results with actual operating data and engineering design information obtained from the SMD electrical network, including bus voltage profiles, generator loading, transformer loading, active and reactive power flows, and network losses. These validation parameters were selected because they represent the principal steady-state performance indicators of the isolated mining power system [27].

To quantitatively assess the fidelity of the developed ETAP model, the base-case load-flow results were compared with the available SMD field measurements and operating reference data. The mine provided instantaneous transformer-loading measurements for the existing electrical network, while nominal bus voltages and generator ratings were obtained from the plant engineering documentation. Where active and reactive power measurements were not separately available, these quantities were reconstructed from the measured apparent power using the operating power factor of 0.85 adopted in the system study. The percentage deviation between the reference and ETAP values was calculated as:

$$\textbf{Deviation (\%)} = \{(\textbf{Reference} - \textbf{ETAP})/\textbf{Reference}\} \times 100 \quad (1)$$

As shown in Table 5, the developed ETAP model demonstrates satisfactory agreement with the available plant operating data. The directly measured transformer-loading deviations range from approximately 1.23% to 9.48%, while the principal bus-voltage deviations remain below 4%. The reconstructed reactive-power flow differs by approximately 2.81%, whereas the active-power-flow deviation is approximately 12.16%. The comparatively larger active-power deviation is attributable to the instantaneous nature of the field measurements and to modelling assumptions required for loads that were unavailable or operating at very low levels during the site measurement campaign. The ETAP power balance fur-

DOI: 10.4236/cs.2026.175005

ther indicates approximately 27 kW of active network losses for the evaluated existing OHL section. Overall, the comparison confirms that the model reproduces the principal voltage profile, equipment loading, generator dispatch, and power-flow characteristics with sufficient engineering fidelity for the subsequent photovoltaic integration studies.

Table 5. quantitative validation of the ETAP base-case model.

Validation parameter	Reference basis	Measured/Reference	ETAP simulation	Deviation
Main 6.6 kV bus voltage	Nominal operating value	6.60 kV	6.70 kV	0.0152
Existing OHL 22 kV bus voltage	Nominal operating value	22.00 kV	22.80 kV	0.0364
Existing 6.6/22 kV OHL transformer loading	Field measurement	2881 kVA	2608 kVA	0.0948
Base Vie transformer loading	Field measurement	547.5 kVA	568 kVA	0.0374
UG Office transformer loading	Field measurement	65.2 kVA	66 kVA	0.0123
Existing OHL active power flow	Derived from measured 2881 kVA, PF = 0.85	2448.9 kW	2151 kW	0.1216
Existing OHL reactive power flow	Derived from measured 2881 kVA, PF = 0.85	1517.7 kvar	1475 kvar	0.0281
UG generator output	Rated/operating reference	2.00 MW	1.784 MW	0.108
Existing OHL active network losses	ETAP power balance	—	≈27 kW	N/A

For model acceptance, the ETAP simulation was considered adequately validated when the deviation between the simulated and available plant operating data remained within engineering tolerances adopted for industrial power-system studies. Bus-voltage deviations below 5%, transformer-loading deviations below 10%, and active/reactive power-flow deviations below 15% were considered acceptable. As shown in Table 1, all validation parameters satisfied these acceptance criteria, confirming that the developed ETAP model accurately reproduces the steady-state operating characteristics of the existing SMD electrical network and provides a reliable basis for subsequent renewable integration studies.

4.6. Simulation Assumptions

To ensure consistency, repeatability, and realistic representation of the isolated mining microgrid, all ETAP simulations were performed under a common set of engineering assumptions. The electrical network was assumed to operate under balanced three-phase conditions with all equipment functioning within its rated operating limits. System frequency and nominal bus voltages were maintained at 50 Hz and their respective rated values unless disturbed during dynamic simulation scenarios [29].

Unless otherwise specified, all transient and protection studies were performed using the operating conditions summarized in Table 2. The Battery Energy Storage System (BESS) was modelled with a rated power of 5 MW, an energy capacity of 10 MWh, and an initial State of Charge (SOC) of 60%. The photovoltaic plant was represented as a grid-following inverter operating under active-power priority with Volt/VAR control, while the three online Mitsubishi synchronous diesel generators remained the grid-forming sources providing voltage and frequency reference throughout all simulations.

The proposed 15 MW photovoltaic power plant was modelled under standard operating conditions using the inverter parameters presented in **Table 1**, while advanced inverter control functions including active power control, Volt/VAR regulation, frequency droop response, low-voltage ride-through (LVRT), high-voltage ride-through (HVRT), and fault-current limitation were implemented where applicable. Unless otherwise specified for individual study scenarios, the existing protection relay settings, transformer tap positions, and network topology remained unchanged to provide a consistent basis for comparing the diesel-only and hybrid diesel-PV operating conditions [30].

All electrical calculations were performed in accordance with internationally recognized engineering standards, including IEC 60909 for short-circuit analysis, IEEE 519 for harmonic assessment, IEEE 1547 for distributed energy resource interconnection, IEC 61000 for power quality evaluation, and IEC 60255 for protection system performance. These assumptions ensure that the simulation results are technically consistent, reproducible, and representative of the operating characteristics of a real isolated mining microgrid [31].

5. Simulation Results and Analysis

5.1. Simulation Strategy

Comprehensive steady-state and dynamic simulations were performed using ETAP Version 22.5 to evaluate the technical performance of integrating a 15 MW photovoltaic (PV) power plant into the isolated SMD mining microgrid. A comparative Before-After assessment methodology was adopted, whereby the existing diesel-only network was first validated and subsequently analyzed following the integration of photovoltaic generation, advanced inverter control functions, and an optional Battery Energy Storage System (BESS). The simulation program comprised load-flow, transient stability, short-circuit, protection coordination, harmonic, and renewable intermittency analyses to evaluate system performance under representative operating conditions. All studies were conducted in accordance with relevant IEC and IEEE standards to ensure the technical reliability, reproducibility, and practical applicability of the results [31] [32].

Unless otherwise stated, all simulation results presented in Sections 5.2 - 5.6 were obtained using the operating conditions summarized in **Table 2**, ensuring a consistent basis for comparing the diesel-only, diesel-PV, diesel-PV with Volt/VAR control, and diesel-PV-BESS operating scenarios.

5.2. Load Flow Analysis

The load-flow simulation results evaluate the steady-state performance of the proposed 15 MW PV integration into the isolated SMD mining microgrid. **Figures**

1-5 compare the diesel-only and hybrid diesel-PV operating conditions, highlighting the effects of PV integration on power factor, voltage profile, active and reactive power flow, and diesel generator loading. The results provide a comprehensive assessment of the technical benefits of photovoltaic integration under normal operating conditions. Three operating cases were analysed: diesel-only, diesel + 15 MW PV, and diesel + PV with Volt/VAR control [33].

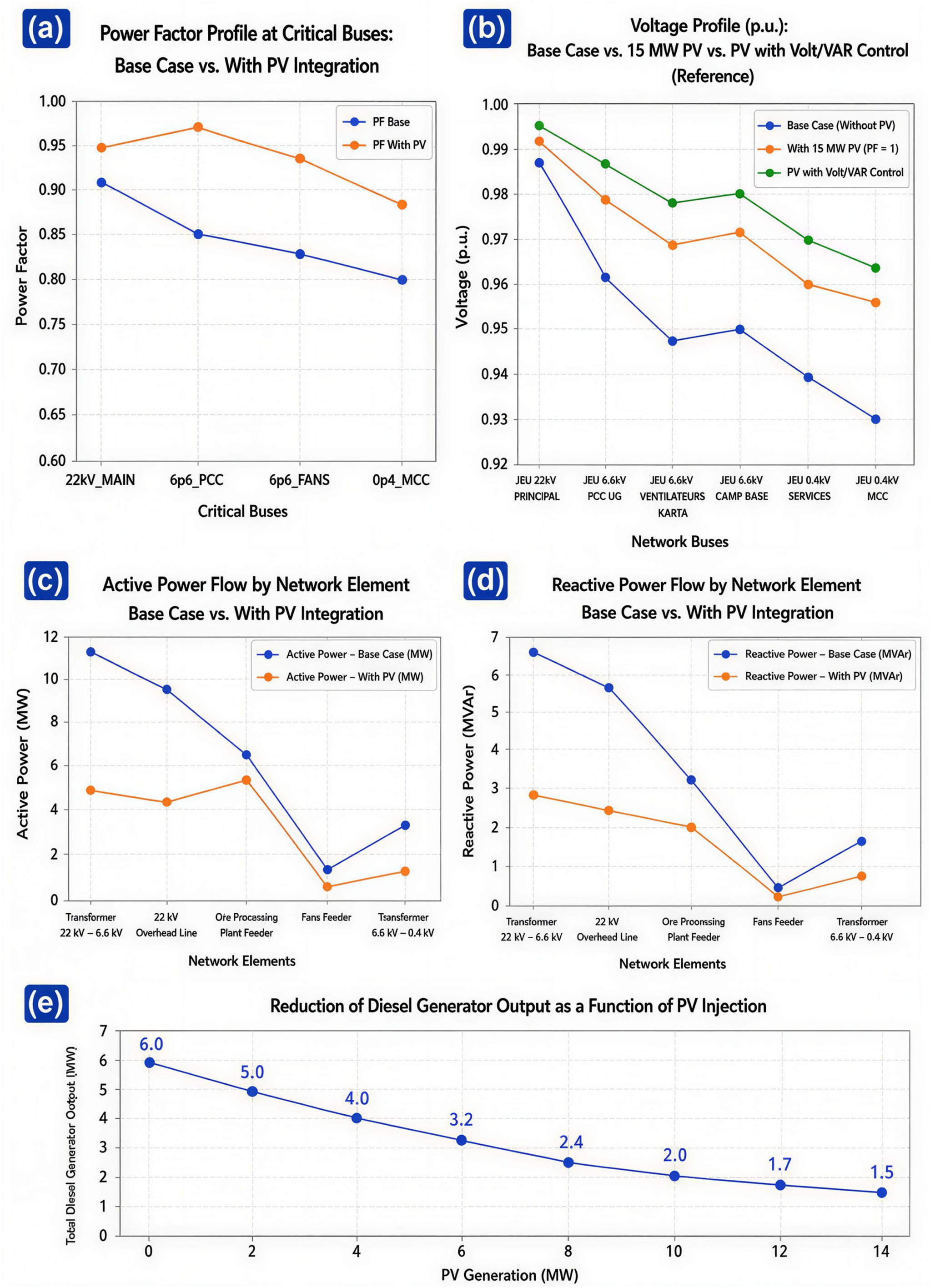

Figure 3. Load flow performance of the hybrid diesel-PV microgrid.

Load flow simulations were performed using ETAP to evaluate the steady-state performance of the isolated SMD/Nordgold power system under three operating scenarios: the diesel-only base case, the integration of a 15 MW photovoltaic (PV) power plant, and PV operation with Volt/VAR control. The results demonstrate that PV integration significantly enhances the electrical performance of the mining network by improving the power factor at critical buses, as shown in **Figure 3(a)**, improving voltage regulation, reducing active and reactive power flows through upstream network components, and optimizing diesel generator dispatch. In the diesel-only configuration, bus voltages progressively decrease from the 22 kV main bus to the 6.6 kV and 0.4 kV distribution levels due to the high reactive power demand of large motor-driven loads, as illustrated in **Figure 3(b)** [34].

The addition of the 15 MW PV plant increases voltage levels by approximately 2% - 3%, while the implementation of Volt/VAR control maintains bus voltages close to the recommended operating range through effective local reactive power support (**Figure 3(b)**). Simultaneously, the PV plant reduces active power transfer through the main transformer, 22 kV overhead line, and downstream feeders (**Figure 3(c)**), while a corresponding reduction in reactive power flow is observed in **Figure 3(d)**. These effects contribute to lower diesel generator loading, reduced network losses, and improved overall power factor, particularly at the medium-voltage buses (**Figure 3(a)**) [35].

The load-flow results indicate a progressive reduction in diesel generator output as photovoltaic generation increases, as shown in **Figure 3(e)**. In all simulation cases, the dispatched diesel generation remained within the installed capacity of the online generating units while maintaining the required spinning reserve for stable isolated microgrid operation.

Overall, **Figures 3(a)-(e)** demonstrate that integrating a 15 MW PV plant with advanced inverter-based reactive power control substantially improves the steady-state efficiency, voltage performance, power factor, and operational reliability of the isolated mining power system while reducing upstream power transfer, diesel generation, fuel consumption, greenhouse gas emissions, and operating costs [36].

5.3. Transient Stability Analysis

Throughout all transient simulations, the synchronous diesel generators remained the primary grid-forming sources, while the photovoltaic inverter and optional BESS operated in coordinated grid-following mode. Consequently, voltage and frequency regulation were established by the diesel generator AVRs and governors, whereas the PV inverter supplied active and reactive power and the BESS provided supplementary Fast Frequency Response (FFR) and synthetic inertia during transient disturbances.

Transient stability simulations were conducted to evaluate the dynamic response of the proposed 15 MW PV-integrated diesel microgrid under representative disturbance scenarios. **Figures 1-5** illustrate the system response in terms of rotor angle oscillations, system frequency, generator load sharing, PCC voltage recovery, and frequency response with and without Battery Energy Storage System (BESS) support. The results demonstrate the ability of the hybrid microgrid to maintain synchronism, rapidly restore voltage and frequency, effectively balance generation following PV power variations, and ensure stable and reliable operation under islanded conditions [33] [34].

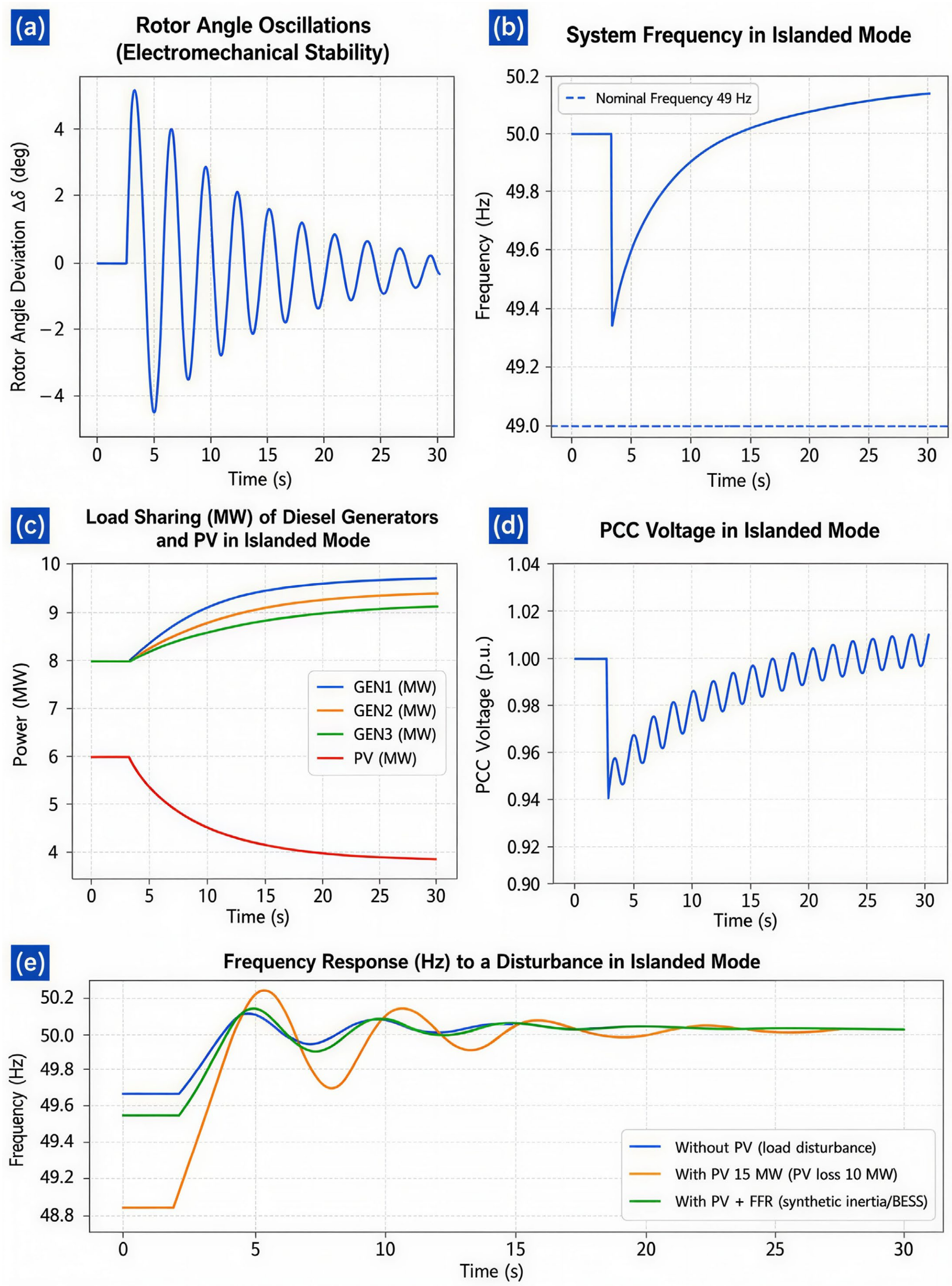

Figure 4. Transient stability performance of the hybrid diesel-PV microgrid.

Transient stability simulations were performed using ETAP to evaluate the dynamic response of the isolated SMD/Nordgold diesel-PV power system following severe disturbances, including islanding events, sudden PV power fluctuations, and generation-load imbalances. The analysis assessed rotor angle stability, system frequency, generator load sharing, PCC voltage recovery, and the effectiveness of fast frequency response (FFR) support. Following the disturbance, the synchronous diesel generators exhibited damped rotor angle oscillations without loss of synchronism, confirming satisfactory electromechanical stability, as shown in Figure 4(a).

System frequency experienced a temporary decline but subsequently recovered toward its nominal operating value through governor action, demonstrating adequate system inertia and spinning reserve, as illustrated in Figure 4(b). During PV power reduction, the diesel generators automatically increased their output through droop control, achieving stable load sharing and a new operating equilibrium without unstable oscillations, as shown in Figure 4(c). Similarly, the PCC voltage underwent a transient dip followed by damped oscillations before stabilizing close to 1 p.u., indicating effective automatic voltage regulator (AVR) performance and robust voltage regulation, as presented in Figure 4(d) [35].

Comparative frequency response analysis further showed that integrating a 15 MW PV plant increases frequency deviations due to reduced system inertia; however, the implementation of Fast Frequency Response (FFR) through synthetic inertia or a Battery Energy Storage System (BESS) significantly improves the frequency nadir, accelerates damping, and shortens the recovery time, as demonstrated in Figure 4(e) [36].

Overall, Figures 4(a)-(e) demonstrate that the proposed diesel-PV hybrid system maintains satisfactory transient stability under the simulated disturbances, while the addition of FFR/BESS substantially enhances the dynamic performance and operational security of the isolated mining power network.

To provide a quantitative assessment of the transient performance of the proposed hybrid diesel-PV microgrid, the principal dynamic response indicators obtained from the ETAP simulations are summarized in Table 6. The reported parameters include the disturbance type, disturbance magnitude, fault location, fault-clearing time, frequency nadir, Rate of Change of Frequency (RoCoF), minimum PCC voltage, maximum rotor-angle deviation, and settling time. These numerical results provide a reproducible basis for evaluating system stability under representative operating disturbances.

To complement the qualitative discussion, the principal transient-performance indices obtained from the ETAP simulations are summarized in Table 6. These numerical results quantify the dynamic response of the hybrid diesel-PV microgrid under the investigated disturbance scenarios and provide a reproducible engineering basis for evaluating system stability. The investigated disturbances included a sudden 10 MW photovoltaic generation loss at the 6.6 kV Point of Common Coupling (PCC) and a three-phase short circuit applied at the PCC, cleared after 200 ms by the protection system.

Table 6. Quantitative transient-performance results for the investigated disturbances.

Parameter	Sudden PV loss	Three-phase fault	PV loss with BESS (FFR)
Disturbance magnitude	10 MW PV trip	35 kA	10 MW PV trip
Fault location	6.6 kV PCC (PV connection)	PCC	6.6 kV PCC
Clearing time	N/A	200 ms	N/A
Frequency nadir (Hz)	49.3	49.3	49.55
Minimum voltage (p.u.)	0.94	0.25	0.98
Maximum rotor angle (˚)	±4.8	Stable (No loss of synchronism)	±3.5
Settling time (s)	≈20	≈1.5	≈10
RoCoF	See discussion below	N/A	Lower than PV-only case

The quantitative results confirm that the hybrid diesel-PV microgrid remains transiently stable for all investigated disturbances. Following the sudden loss of 10 MW of photovoltaic generation, the system frequency decreases to a minimum value of approximately 49.3 Hz, while the PCC voltage reaches approximately 0.94 p.u. before recovering to its nominal value. The maximum rotor-angle deviation remains limited to approximately ±5˚, indicating that synchronism is preserved throughout the disturbance. During the simulated three-phase short circuit applied at the PCC, the fault current reaches approximately 35 kA, and the protection system successfully clears the fault within 200 ms, resulting in rapid voltage recovery without generator instability. When Fast Frequency Response (FFR) from the BESS is enabled, the frequency nadir improves to approximately 49.55 Hz, rotor-angle oscillations are more effectively damped, and the settling time is reduced from approximately 20 s to 10 s, demonstrating the beneficial contribution of synthetic inertia and rapid active-power support.

5.4. Hybrid Microgrid Transient Stability

The transient stability simulations evaluate the dynamic performance of the proposed 15 MW PV-integrated hybrid diesel microgrid under representative operating disturbances. Figures 1-6 present the system response in terms of Rate of Change of Frequency (RoCoF), governor primary response, BESS state of charge, PV ramp-rate control, fault current characteristics, circuit breaker operation, PCC voltage recovery, and protection coordination. These results provide a comprehensive assessment of the hybrid microgrid's ability to withstand disturbances, rapidly restore system stability, and maintain reliable and secure operation under high photovoltaic penetration [32]-[36].

The above figures present the transient stability performance of the proposed hybrid diesel-PV microgrid under dynamic operating conditions. The simulations evaluate the system response to rapid PV generation loss, frequency disturbances, three-phase faults, and protection system operation. Figure 5(a) presents the Rate of Change of Frequency (RoCoF) following rapid PV loss, while Figure 5(b) illustrates the corresponding primary frequency response provided by the diesel generator governor.

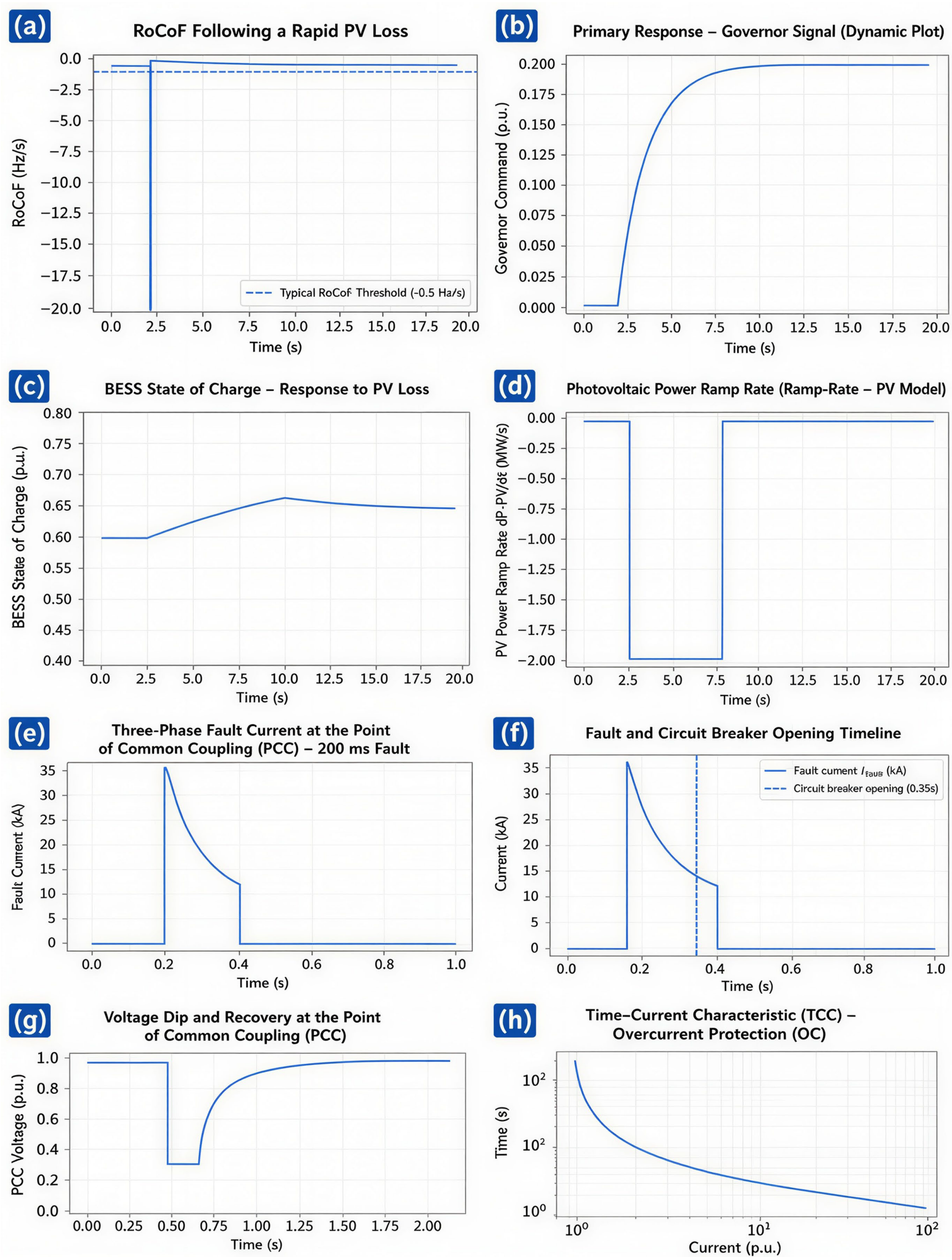

Figure 5. Dynamic stability of the hybrid diesel-PV-BESS microgrid.

The instantaneous RoCoF plot presented in Figure 5(a) corresponds to the numerical derivative calculated immediately after the imposed disturbance. This value represents the instantaneous simulation response rather than the filtered RoCoF evaluated by practical protection relays. Modern numerical relays estimate RoCoF using moving measurement windows and digital filtering, thereby significantly attenuating the initial spike. Consequently, the instantaneous excursion shown in the simulation should not be directly compared with the relay operating threshold of −0.5 Hz/s. The protection assessment presented in this study is therefore based on the filtered RoCoF response rather than on the instantaneous numerical derivative. The BESS supplies short-term dynamic support, maintaining an adequate state of charge and improving frequency stability during transient events, as shown in Figure 5(c). The PV ramp-rate control effectively limits sudden power fluctuations, thereby reducing the impact on diesel generators and network frequency, as illustrated in Figure 5(d).

Short-circuit simulations demonstrate the three-phase fault-current response at the PCC, as presented in Figure 5(e), and a rapid interruption of the fault following circuit breaker operation, as shown in Figure 5(f). The PCC voltage subsequently recovers quickly after fault clearance, confirming satisfactory voltage stability, as illustrated in Figure 5(g). The time-current characteristic (TCC) in Figure 5(h) verifies proper coordination of the overcurrent protection system, ensuring selective and reliable fault isolation.

Protection coordination simulations were carried out using the existing SMD overcurrent relay settings implemented in the ETAP model. The coordination assessment, represented by the fault-clearing sequence in Figure 5(f) and the TCC characteristic in Figure 5(h), verified relay selectivity, breaker operating sequence, and fault-clearing performance for the adopted fault scenarios, confirming correct discrimination between primary and backup protection devices.

Overall, Figures 5(a)-(h) demonstrate that the proposed 15 MW PV-integrated diesel microgrid exhibits satisfactory transient stability, effective protection coordination, rapid fault recovery, and robust dynamic performance, confirming its suitability for reliable operation in an isolated mining power system with high renewable energy penetration [37] [38].

5.5. Harmonic Analysis

Harmonic simulations were conducted to evaluate the power quality performance of the proposed 15 MW PV-integrated hybrid microgrid under normal operating conditions. Figures 1-6 present the results for current harmonic distortion (THDi), network resonance characteristics, voltage harmonic spectrum, filter effectiveness, and comparative total harmonic voltage distortion (THDv) before and after PV integration. The analysis provides a comprehensive assessment of the impact of photovoltaic generation on harmonic performance and verifies compliance with IEEE Std. 519 through the application of appropriate harmonic mitigation measures [38].

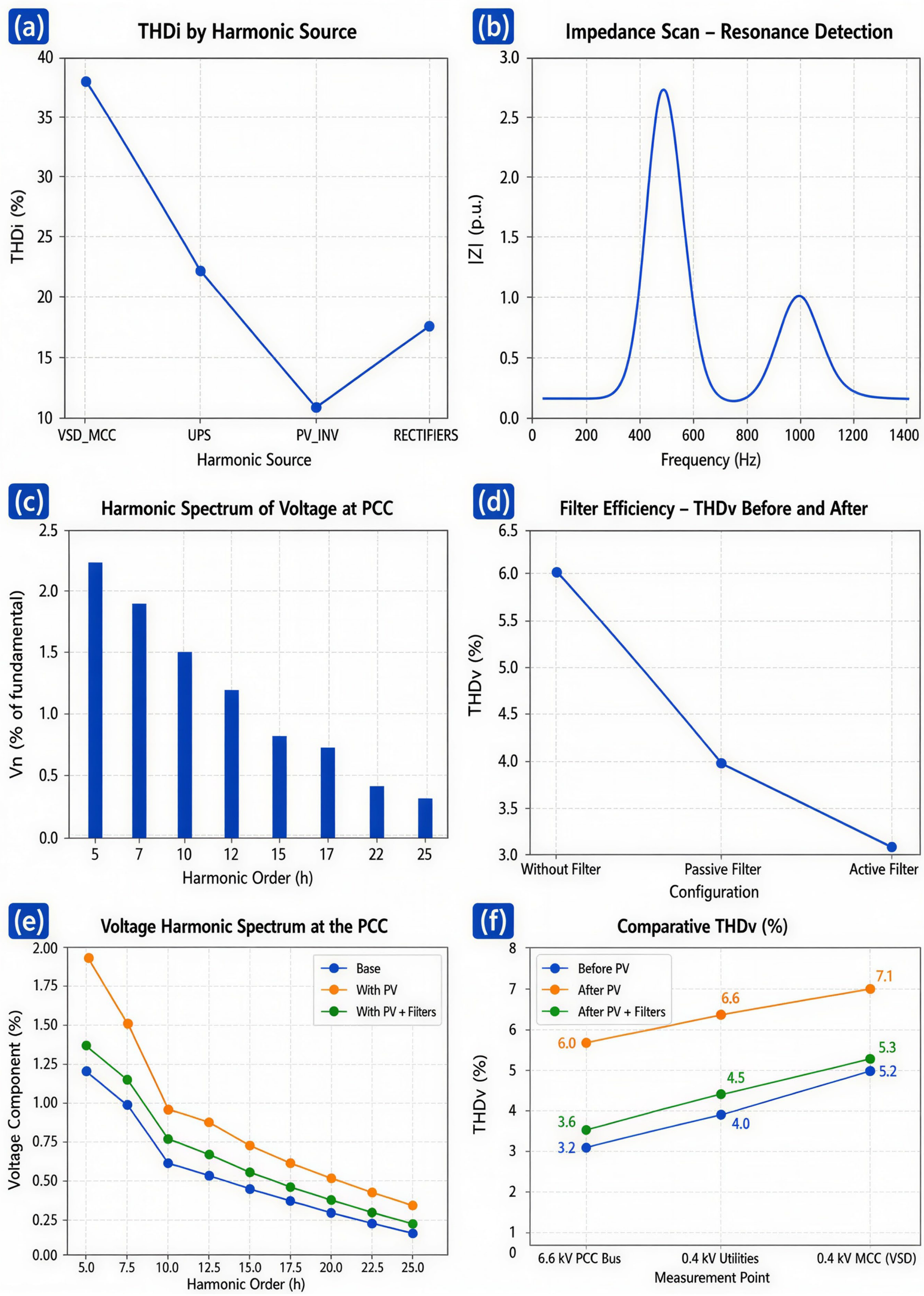

Figure 6. Harmonic performance of the hybrid diesel-PV microgrid.

Harmonic analysis was conducted using ETAP to evaluate the impact of integrating a 15 MW photovoltaic (PV) power plant on power quality and compliance with IEEE 519 and IEC 61000 standards. The assessment included current harmonic distortion (THDi) of major nonlinear loads (**Figure 6(a)**), impedance scanning for resonance identification (**Figure 6(b)**), voltage harmonic spectrum analysis at the point of common coupling (PCC) (Figure 6(c) and Figure 6(e)), and the effectiveness of harmonic mitigation techniques (Figure 6(d) and Figure 6(f)).

The results indicate that variable speed drives (VSDs) are the dominant harmonic sources, exhibiting the highest current distortion, followed by UPS systems and rectifiers, whereas the PV inverter contributes comparatively lower harmonic distortion due to its advanced PWM control and integrated LCL filtering, as shown in Figure 6(a). Impedance scan analysis (Figure 6(b)) identified potential resonance frequencies around 500 - 600 Hz and at higher frequencies around 1000 Hz, highlighting the need to prevent harmonic amplification under certain network operating conditions.

The voltage harmonic spectrum at the PCC (Figure 6(c)) shows that the lower-order harmonic components are dominant, with their magnitude progressively decreasing at higher harmonic orders. The comparative harmonic spectrum (Figure 6(e)) further illustrates the effect of PV integration on individual voltage harmonic components and the subsequent reduction achieved through harmonic filtering. Nevertheless, the overall voltage distortion remains within acceptable limits, indicating that no significant resonance amplification occurs under normal operating conditions. Furthermore, Figure 6(d) demonstrates that passive and active harmonic filters substantially reduce the total harmonic voltage distortion (THDv), while Figure 6(f) compares THDv at the 6.6 kV PCC bus, 0.4 kV utilities, and 0.4 kV MCC before PV integration, after PV integration, and after the application of harmonic filters. These results demonstrate that appropriate filtering significantly improves power quality and supports compliance with international harmonic standards.

Overall, Figures 6(a)-(f) demonstrate that the proposed diesel-PV hybrid microgrid maintains satisfactory harmonic performance when appropriate filtering and resonance-mitigation measures are implemented. The resulting harmonic distortion at the PCC remains within acceptable power-quality limits, supporting reliable system operation and compliance with the applicable requirements of IEEE Std 519 and IEC 61000 [36] [37].

5.6. Performance Evaluation

The technical performance of the proposed hybrid diesel-PV power system was evaluated using a comprehensive set of electrical performance indicators to quantify the impact of integrating a 15 MW photovoltaic power plant into the isolated SMD mining microgrid. Comparative assessments were performed between the reference diesel-only configuration and the hybrid operating scenarios to evaluate both steady-state and dynamic system behavior.

The principal evaluation criteria included bus voltage magnitude (p.u.), active and reactive power flow (MW/MVAr), generator loading (%), system frequency (Hz), Rate of Change of Frequency (RoCoF), rotor angle stability, short-circuit current (kA), relay operating time (ms), total harmonic voltage distortion (THDv), and total harmonic current distortion (THDi). Additional indicators, including network losses, power factor, diesel fuel displacement, and renewable energy penetration, were also considered to assess the overall operational efficiency and reliability of the hybrid microgrid.

The simulation results were benchmarked against the relevant requirements of IEC 60909, IEEE 519, IEEE 1547, IEC 61000, and IEC 60255 to verify compliance with internationally accepted limits for system stability, protection coordination, and power quality. The comparative analysis enabled a comprehensive assessment of the technical feasibility, operational reliability, and resilience of the proposed diesel-PV hybrid system under both normal operating conditions and severe network disturbances, providing quantitative engineering evidence to support the large-scale integration of photovoltaic generation into isolated mining microgrids [38] [39].

6. Results and Discussion

The comprehensive ETAP simulations demonstrate that integrating a 15 MW photovoltaic (PV) power plant into the isolated SMD/Nordgold mining microgrid is technically feasible and substantially enhances the electrical performance, operational efficiency, and sustainability of the existing diesel-based power system. Comparative analyses between the reference diesel-only configuration and the proposed hybrid diesel-PV microgrid consistently indicate that high renewable energy penetration can be achieved without compromising electrical stability, protection performance, or power quality when appropriate inverter control strategies and energy storage support are implemented [39].

Under steady-state operating conditions, PV integration improved voltage regulation throughout the medium- and low-voltage network by providing local active power generation and reactive power support through Volt/VAR control. The resulting reduction in active and reactive power transfer through upstream transformers and distribution feeders decreased network losses, improved the overall power factor, and significantly reduced diesel generator loading. These improvements demonstrate the ability of distributed photovoltaic generation to increase system efficiency while reducing fuel consumption, operating costs, and greenhouse gas emissions, thereby supporting the decarbonization objectives of isolated mining operations [40].

Dynamic simulations confirmed that the proposed hybrid diesel-PV microgrid maintains satisfactory transient stability under severe operating disturbances. Following generation-load imbalances and sudden reductions in photovoltaic output, the synchronous diesel generators remained synchronized and exhibited well-damped rotor-angle oscillations, while the automatic voltage regulators and governor control systems restored voltage and frequency to acceptable operating limits. Although increased photovoltaic penetration reduced the effective rotational inertia of the system, the implementation of a Battery Energy Storage System (BESS) providing Fast Frequency Response (FFR) significantly enhanced dynamic performance by reducing the Rate of Change of Frequency (RoCoF), improving the frequency nadir, shortening recovery time, and mitigating the impact of renewable intermittency. The transient-performance indices summarized in **Table 6** further demonstrate that the proposed hybrid system maintained a minimum frequency of approximately 49.3 Hz, a minimum PCC voltage of 0.94 p.u., rotor-angle deviations below ±5˚, and successful fault clearance within 200 ms under the investigated disturbances, confirming compliance with the transient stability objectives established for the study.

These results confirm that coordinated inverter controls and fast-acting energy storage are essential for maintaining frequency resilience in isolated mining microgrids with high renewable penetration [41].

Short-circuit and protection studies demonstrated that inverter-based photovoltaic generation moderately reduced fault-current levels compared with the diesel-only configuration. Nevertheless, the reduction was not sufficient to compromise protection system performance. Minor adjustments to relay pickup settings and coordination margins were adequate to preserve selective fault isolation and reliable circuit-breaker operation. These findings indicate that existing protection schemes can generally accommodate large-scale photovoltaic integration with limited modifications, provided that detailed protection coordination studies are performed during the design stage.

Power quality assessments further showed that the dominant harmonic distortion originated from existing nonlinear industrial loads, particularly variable-speed drives, rather than from the photovoltaic inverter itself. With appropriate passive and active harmonic filtering, both voltage and current harmonic distortion remained within the limits prescribed by IEEE 519, confirming that large-scale photovoltaic integration can be achieved without adversely affecting power quality. This result highlights the importance of harmonic mitigation measures in industrial microgrids containing extensive power electronic equipment.

Overall, the simulation results provide strong engineering evidence that the proposed hybrid diesel-PV architecture represents a technically robust and operationally reliable solution for isolated mining power systems. Beyond reducing diesel fuel consumption and carbon emissions, the integration of advanced inverter controls, coordinated protection, and BESS support enables high renewable energy penetration while maintaining electrical stability, operational security, and compliance with internationally recognised power system standards. These findings demonstrate the practical applicability of the proposed ETAP-based methodology and provide valuable guidance for the planning, design, and implementation of renewable-powered mining microgrids in Africa and other remote industrial regions [41] [42].

7. Engineering Implications

This study provides a practical engineering framework for integrating large-scale photovoltaic (PV) generation into isolated diesel-powered mining microgrids.

The ETAP simulation results demonstrate that high PV penetration can be successfully achieved without compromising system reliability when supported by comprehensive load-flow, transient stability, short-circuit, protection coordination, and harmonic analyses during the design stage. Advanced inverter functions including Volt/VAR control, LVRT/HVRT, frequency droop, and ramp-rate control together with a Battery Energy Storage System (BESS) providing Fast Frequency Response (FFR), significantly enhance voltage regulation, frequency stability, and overall system resilience.

The study also demonstrates that the reduced fault-current contribution of inverter-based generation can be effectively managed through appropriate relay setting adjustments and protection coordination, ensuring secure operation under bidirectional power-flow conditions. Furthermore, the proposed hybrid diesel-PV architecture reduces diesel consumption, network losses, operating costs, and greenhouse gas emissions while maintaining compliance with IEC 60909, IEC 61000, IEEE 519, and IEEE 1547.

The proposed ETAP-based assessment methodology provides a practical reference for mining companies, utilities, consultants, and power system engineers involved in the planning, design, and implementation of reliable, resilient, and sustainable renewable-powered mining microgrids. It also offers valuable engineering guidance for future mining electrification and decarbonization projects in remote regions with high renewable energy penetration [41] [42].

8. Conclusions

This study presented a comprehensive technical assessment of integrating a 15 MW photovoltaic (PV) power plant into the isolated electrical network of the Société Minière de Dinguiraye (SMD) gold mine in Guinea using a high-fidelity ETAP Version 22.5 simulation model. By combining steady-state and dynamic analyses including load-flow, transient stability, photovoltaic dynamic behavior, short-circuit analysis, protection coordination, harmonic assessment, and renewable intermittency studies the research demonstrated the technical feasibility of large-scale photovoltaic integration into an isolated mining microgrid without compromising system security, operational reliability, or power quality.

The simulation results showed that the proposed hybrid diesel-PV configuration significantly improves voltage regulation, power factor, and overall network efficiency while reducing diesel generator loading, active and reactive power transfer, transmission losses, fuel consumption, and associated greenhouse gas emissions. Dynamic analyses confirmed satisfactory rotor-angle stability, effective voltage recovery, and acceptable frequency deviations following severe network disturbances. Furthermore, the integration of a Battery Energy Storage System (BESS) providing Fast Frequency Response (FFR) substantially enhanced system resilience by reducing the Rate of Change of Frequency (RoCoF), improving the frequency nadir, mitigating renewable intermittency, and accelerating post-disturbance frequency recovery. Protection studies demonstrated that only limited relay setting adjustments were required to accommodate the reduced fault-current contribution of inverter-based resources while maintaining adequate protection selectivity and fault-clearing performance. Harmonic analyses further confirmed compliance with IEEE 519 following the application of appropriate harmonic mitigation measures [43] [44].

A major contribution of this research is the development of an integrated ETAP-based engineering framework capable of simultaneously evaluating power-flow performance, transient stability, protection coordination, fault behavior, and power quality within a single validated industrial model. Unlike many previous investigations that consider these aspects independently, the proposed methodology provides a holistic and reproducible approach for assessing renewable energy integration in isolated mining power systems, thereby bridging the gap between academic research and industrial engineering practice [45]. The validated ETAP model satisfied the adopted engineering acceptance criteria for voltage profile, equipment loading, power flow, and protection performance, providing confidence in the reproducibility and applicability of the reported simulation results for future hybrid diesel-PV microgrid studies.

The findings demonstrate that, when supported by advanced inverter control strategies, coordinated protection schemes, and appropriately sized energy storage, large-scale photovoltaic generation can substantially decarbonize isolated mining operations while maintaining compliance with internationally recognized engineering standards. Consequently, the proposed hybrid diesel-PV architecture represents a technically robust, economically attractive, and environmentally sustainable solution for future mining electrification projects.

Future research should extend the present work by incorporating techno-economic optimization, long-term operational scheduling, stochastic solar irradiance modelling, battery degradation analysis, real-time Energy Management Systems (EMS), and Hardware-in-the-Loop (HIL) or field validation to further strengthen the applicability of the proposed methodology for next-generation renewable-powered mining microgrids.

Conflicts of Interest

The authors declare no conflicts of interest regarding the publication of this paper.

References

[1] International Energy Agency (IEA) (2024) Renewables 2024: Analysis and Forecast to 2030. International Energy Agency. https://www.iea.org/reports/renewables-2024

[2] International Renewable Energy Agency (IRENA) (2024) Renewable Power Generation Costs in 2023. IRENA. https://www.irena.org/Publications/2024/Sep/Renewable-Power-Generation-Costs-in-2023

[3] International Council on Mining and Metals (ICMM) (2021) Climate Change Position Statement. ICMM. https://www.icmm.com/en-gb/our-principles/position-statements/climate-change

[4] World Bank (2017) The Growing Role of Minerals and Metals for a Low-Carbon Future. World Bank. https://documents.worldbank.org/en/publication/documents-reports/documentdetail/207371500386458722

[5] Ocon, J.D. and Bertheau, P. (2019) Energy Transition from Diesel-Based to Solar Photovoltaics-Battery-Diesel Hybrid System-Based Island Grids in the Philippines—Techno-Economic Potential and Policy Implication on Missionary Electrification. *Journal of Sustainable Development of Energy, Water and Environment Systems*, **7**, 139-154. https://doi.org/10.13044/j.sdewes.d6.0230

[6] Lasseter, R.H. (2002) MicroGrids. 2002 *IEEE Power Engineering Society Winter Meeting. Conference Proceedings* (*Cat. No.02CH*37309), New York, 27-31 January 2002, 305-308. https://doi.org/10.1109/pesw.2002.985003

[7] Hatziargyriou, N. (ed.) (2014) Microgrids: Architectures and Control. Wiley-IEEE Press.

[8] Kundur, P., Paserba, J., Ajjarapu, V., Andersson, G., Bose, A., Canizares, C., *et al.* (2004) Definition and Classification of Power System Stability. *IEEE Transactions on Power Systems*, **19**, 1387-1401.

[9] Lopes, J.A.P., Moreira, C.L. and Madureira, A.G. (2006) Defining Control Strategies for Microgrids Islanded Operation. *IEEE Transactions on Power Systems*, **21**, 916-924. https://doi.org/10.1109/tpwrs.2006.873018

[10] Pogaku, N., Prodanovic, M. and Green, T.C. (2007) Modeling, Analysis and Testing of Autonomous Operation of an Inverter-Based Microgrid. *IEEE Transactions on Power Electronics*, **22**, 613-625. https://doi.org/10.1109/tpel.2006.890003

[11] Rocabert, J., Luna, A., Blaabjerg, F. and Rodríguez, P. (2012) Control of Power Converters in AC Microgrids. *IEEE Transactions on Power Electronics*, **27**, 4734-4749. https://doi.org/10.1109/tpel.2012.2199334

[12] Bidram, A. and Davoudi, A. (2012) Hierarchical Structure of Microgrids Control System. *IEEE Transactions on Smart Grid*, **3**, 1963-1976. https://doi.org/10.1109/tsg.2012.2197425

[13] Olivares, D.E., Mehrizi-Sani, A., Etemadi, A.H., Canizares, C.A., Iravani, R., Kazerani, M., *et al.* (2014) Trends in Microgrid Control. *IEEE Transactions on Smart Grid*, **5**, 1905-1919. https://doi.org/10.1109/tsg.2013.2295514

[14] Bevrani, H., Ise, T. and Miura, Y. (2014) Virtual Synchronous Generators: A Survey and New Perspectives. *International Journal of Electrical Power & Energy Systems*, **54**, 244-254. https://doi.org/10.1016/j.ijepes.2013.07.009

[15] Kerdphol, T., Fuji, K., Mitani, Y., Watanabe, M. and Qudaih, Y. (2016) Optimization of a Battery Energy Storage System Using Particle Swarm Optimization for Stand-Alone Microgrids. *International Journal of Electrical Power & Energy Systems*, **81**, 32-39. https://doi.org/10.1016/j.ijepes.2016.02.006

[16] Kerdphol, T., Rahman, F.S., Mitani, Y., Watanabe, M. and Küfeoğlu, S. (2018) Robust Virtual Inertia Control of an Islanded Microgrid Considering High Penetration of Renewable Energy. *IEEE Access*, **6**, 625-636. https://doi.org/10.1109/access.2017.2773486

[17] Joung, K.W., Lee, H. and Park, J. (2019) Assessment of Maximum Penetration Capacity of Photovoltaic Generator Considering Frequency Stability in Practical Stand-Alone Microgrid. *Energies*, **12**, Article No. 1445. https://doi.org/10.3390/en12081445

[18] Grover, H., Verma, A. and Bhatti, T.S. (2022) DOBC-Based Frequency & Voltage Regulation Strategy for PV-Diesel Hybrid Microgrid during Islanding Conditions.

Renewable Energy, **196**, 883-900. https://doi.org/10.1016/j.renene.2022.06.140

[19] Youssef, A., Mallah, M., Ali, A., Shaaban, M.F. and Mohamed, E.E.M. (2023) Enhancement of Microgrid Frequency Stability Based on the Combined Power-to-Hydrogen-to-Power Technology under High Penetration Renewable Units. *Energies*, **16**, Article No. 3377. https://doi.org/10.3390/en16083377

[20] Sepasi, S., Talichet, C. and Pramanik, A.S. (2023) Power Quality in Microgrids: A Critical Review of Fundamentals, Standards, and Case Studies. *IEEE Access*, **11**, 108493-108531. https://doi.org/10.1109/access.2023.3321301

[21] Hamanah, W.M., Hossain, M.I., Shafiullah, M. and Abido, M.A. (2023) AC Microgrid Protection Schemes: A Comprehensive Review. *IEEE Access*, **11**, 76842-76868. https://doi.org/10.1109/access.2023.3298306

[22] Oureilidis, K.O. and Demoulias, C.S. (2016) A Fault Clearing Method in Converter-Dominated Microgrids with Conventional Protection Means. *IEEE Transactions on Power Electronics*, **31**, 4628-4640. https://doi.org/10.1109/tpel.2015.2476702

[23] Paquette, A.D. and Divan, D.M. (2015) Virtual Impedance Current Limiting for Inverters in Microgrids with Synchronous Generators. *IEEE Transactions on Industry Applications*, **51**, 1630-1638. https://doi.org/10.1109/tia.2014.2345877

[24] Hussain, M.H., Rahim, S.R.A. and Musirin, I. (2013) Optimal Overcurrent Relay Coordination: A Review. *Procedia Engineering*, **53**, 332-336. https://doi.org/10.1016/j.proeng.2013.02.043

[25] Lyu, M., Wu, G., Rao, Z., Zheng, J., Zhang, C., Huang, S., *et al.* (2021) Predictive Cascaded Speed and Torque Control for a Novel Three-Modular Three-Phase PMSM. *International Journal of Electrical Power & Energy Systems*, **129**, Article ID: 106798. https://doi.org/10.1016/j.ijepes.2021.106798

[26] ETAP (2026) ETAP Electrical Power System Analysis Software: Product Documentation. Operation Technology, Inc. https://etap.com

[27] IEEE (2018) IEEE Standard for Interconnection and Interoperability of Distributed Energy Resources with Associated Electric Power Systems Interfaces, IEEE Std 1547-2018. IEEE.

[28] International Electrotechnical Commission (IEC) (2004) IEC 61727: Photovoltaic Systems-Characteristics of the Utility Interface. IEC. https://webstore.iec.ch/en/publication/5736

[29] IEEE (2022) IEEE Recommended Practice and Requirements for Harmonic Control in Electric Power Systems, IEEE Std 519-2022. IEEE.

[30] International Electrotechnical Commission (IEC) (2016) IEC 60909-0: Short-Circuit Currents in Three-Phase AC Systems—Part 0: Calculation of Currents. IEC. https://webstore.iec.ch/en/publication/24100

[31] International Electrotechnical Commission (IEC) (2015) IEC 61000-4-30: Electromagnetic Compatibility-Part 4-30: Testing and Measurement Techniques-Power Quality Measurement Methods. IEC. https://webstore.iec.ch/en/publication/21844

[32] International Electrotechnical Commission (IEC) (2022) IEC 60255-1: Measuring Relays and Protection Equipment-Part 1: Common Requirements. IEC. https://webstore.iec.ch/en/publication/59762?utm_source=chatgpt.com

[33] International Electrotechnical Commission (IEC) (2013) IEC 61850-1: Communication Networks and Systems for Power Utility Automation-Part 1: Introduction and Overview. IEC. https://webstore.iec.ch/en/publication/6007

[34] International Electrotechnical Commission (IEC) (2022) IEC 60034-1: Rotating Electrical Machines-Part 1: Rating and Performance. IEC.

https://webstore.iec.ch/en/publication/65446

[35] Arrillaga, J. and Watson, N.R. (2003) Power System Harmonics. 2nd Edition, John Wiley & Sons. https://doi.org/10.1002/0470871229

[36] Bollen, M.H.J. (2000) Understanding Power Quality Problems: Voltage Sags and Interruptions. IEEE Press.

[37] Dugan, R.C., McGranaghan, M.F., Santoso, S. and Beaty, H.W. (2012) Electrical Power Systems Quality. 3rd Edition, McGraw-Hill Education. https://www.accessengineeringlibrary.com/content/book/9780071761550

[38] Horowitz, S.H. and Phadke, A.G. (2014) Power System Relaying. 4th Edition, Wiley.

[39] Guerrero, J.M., Vasquez, J.C., Matas, J., de Vicuña, L.G. and Castilla, M. (2011) Hierarchical Control of Droop-Controlled AC and DC Microgrids—A General Approach toward Standardization. *IEEE Transactions on Industrial Electronics*, **58**, 158-172. https://doi.org/10.1109/tie.2010.2066534

[40] Savaghebi, M., Jalilian, A., Vasquez, J.C. and Guerrero, J.M. (2012) Secondary Control for Voltage Quality Enhancement in Microgrids. *IEEE Transactions on Smart Grid*, **3**, 1893-1902. https://doi.org/10.1109/tsg.2012.2205281

[41] Shafiee, Q., Guerrero, J.M. and Vasquez, J.C. (2014) Distributed Secondary Control for Islanded Microgrids—A Novel Approach. *IEEE Transactions on Power Electronics*, **29**, 1018-1031. https://doi.org/10.1109/tpel.2013.2259506

[42] Coban, H.H., Rehman, A. and Mousa, M. (2022) Load Frequency Control of Microgrid System by Battery and Pumped-Hydro Energy Storage. *Water*, **14**, Article No. 1818. https://doi.org/10.3390/w14111818

[43] Chauhan, A., Upadhyay, S., Khan, M.T., Hussain, S.M.S. and Ustun, T.S. (2021) Performance Investigation of a Solar Photovoltaic/Diesel Generator Based Hybrid System with Cycle Charging Strategy Using BBO Algorithm. *Sustainability*, **13**, Article No. 8048. https://doi.org/10.3390/su13148048

[44] Marqusee, J., Becker, W. and Ericson, S. (2021) Resilience and Economics of Microgrids with PV, Battery Storage, and Networked Diesel Generators. *Advances in Applied Energy*, **3**, Article ID: 100049. https://doi.org/10.1016/j.adapen.2021.100049

[45] Khosravi, N., Çelik, D., Bevrani, H. and Echalih, S. (2025) Microgrid Stability: A Comprehensive Review of Challenges, Trends, and Emerging Solutions. *International Journal of Electrical Power & Energy Systems*, **170**, Article ID: 110829. https://doi.org/10.1016/j.ijepes.2025.110829